

Energy Transfer

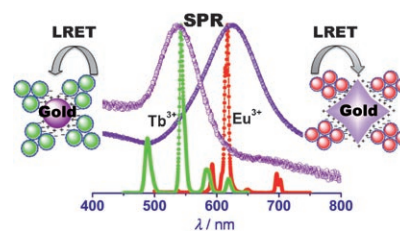
J.-Q. Gu, L.-D. Sun,* Z.-G. Yan,
C.-H. Yan*

Luminescence Resonance Energy
Transfer Sensors Based on the
Assemblies of Oppositely Charged
Lanthanide/Gold Nanoparticles in
Aqueous Solution

Chem. Asian J.

DOI: 10.1002/asia.200800230

Opposites attract: This work demonstrates luminescence resonance energy transfer sensors based on $\text{YVO}_4\text{:Eu/LaPO}_4\text{:Ce,Tb}$ nanoparticles as donors and differently shaped gold nanoparticles as acceptors, combined through the electrostatic interactions between the oppositely charged nanoparticles.



Artificial Cells

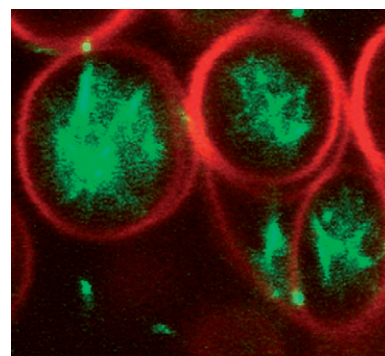
D. Merkle,* N. Kahya, P. Schwille*

Reconstitution and Anchoring of
Cytoskeleton inside Giant Unilamellar
Vesicles

ChemBioChem

DOI: 10.1002/cbic.200800340

An artificial anchor? A critical step in achieving artificial cell replication would be to construct and encapsulate machinery that constrict and divide a cell-like compartment. By extracting integral membrane proteins and lipids from porcine brain, we grew giant unilamellar vesicles (GUVs) that encapsulate polymerised actin and spectrin/ankyrin. In the presence of spectrin/ankyrin, the actin filaments formed tight bundles that often localized and immobilized to the interior walls of the GUVs.



Surface Chemistry

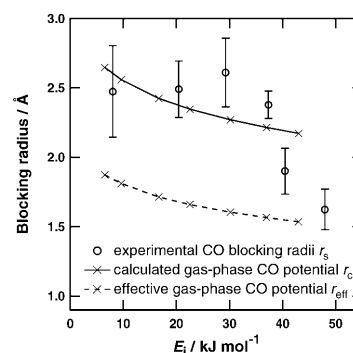
H. Ueta, I. M. N. Groot, M. A. Gleeson,
S. Stolte, G. C. McBane,
L. B. F. Juurlink, A. W. Kleyne*

CO Blocking of D_2 Dissociative
Adsorption on Ru(0001)

ChemPhysChem

DOI: 10.1002/cphc.200800294

CO poisons surface reactivity: Dissociative adsorption of D_2 on Ru(0001) is blocked by pre-adsorption of CO molecules. The dependence of CO blocking radius on D_2 kinetic energy (see picture) shows a behaviour that differs markedly from that of a simple steric model. The results suggest that a CO-induced barrier for D_2 dissociation exists in the vicinity of CO molecules, and at high CO coverage all D_2 dissociation occurs via this barrier.



Molecular Modeling

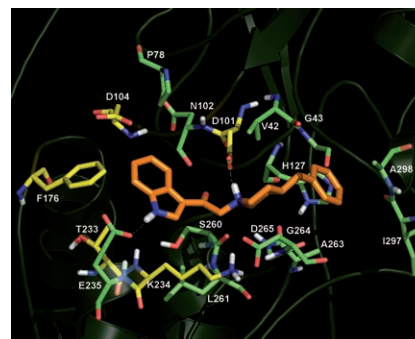
R. Gitto, L. De Luca, S. Ferro,
F. Occhiuto, S. Samperi, G. De Sarro,
E. Russo, L. Ciranna, L. Costa,
A. Chimirri*

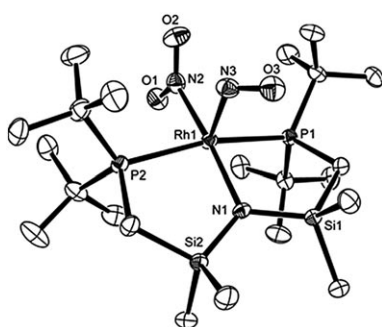
Computational Studies to Discover a
New NR2B/NMDA Receptor Antagonist
and Evaluation of Pharmacological
Profile

ChemMedChem

DOI: 10.1002/cmdc.200800124

Theory and practice: A ligand-based and target-based approach was combined for the discovery of new ligands for the ionotropic glutamate NMDA/NR2B receptor. The identification of hits and evaluation of their neuroprotective effects in in vivo and in vitro experiments is reported.





This work establishes the fate of binding one radical (NO) to an even-electron rhodium, and shows the primary product of a 1:1 collision to be a member of the growing class of "half-bent" MNO complexes.

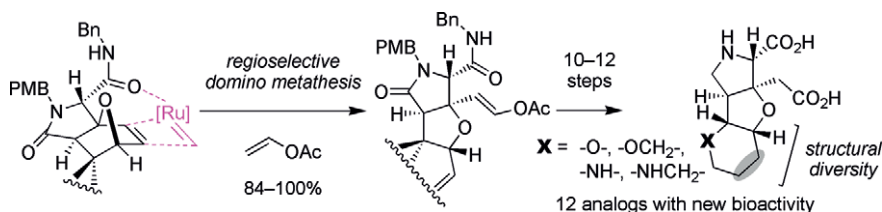
Fate of Radicals

A. Y. Verat, M. Pink, H. Fan,
B. C. Fullmer, J. Telser, K. G. Caulton*

Reactivity of the Radical NO with a Masked Form of 14 Valence Electron (PNP)Rh: Forming Rh(0, I or II)?

Eur. J. Inorg. Chem.

DOI: 10.1002/ejic.200800256



Twelve artificial glutamate analogues inspired by natural products were efficiently synthesized by employing a regioselective domino metathesis reaction of

7-oxanorbornenes as the key step. One analogue was found to exhibit unique hypoaquity.

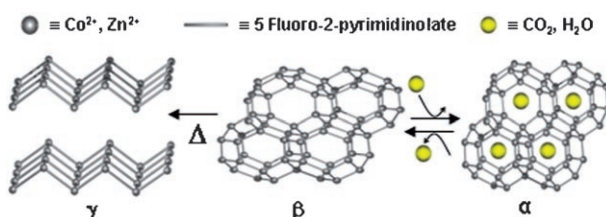
Bioactive Glutamate Analogues

M. Ikoma, M. Oikawa,* M. B. Gill,
G. T. Swanson, R. Sakai, K. Shimamoto,
M. Sasaki

Regioselective Domino Metathesis of 7-Oxanorbornenes and Its Application to the Synthesis of Biologically Active Glutamate Analogues

Eur. J. Org. Chem.

DOI: 10.1002/ejoc.200800704



Flexible MOFs! Application of high-pressure CO₂ or exposure to moisture of a zeomimetic coordination network induces a reversible structural change from a non-porous β -phase to a porous

α -phase (see figure). An additional structural transformation into a layered γ -phase is promoted by thermal treatment implying a concomitant modification of the physicochemical properties.

Coordination Chemistry

S. Galli,* N. Masciocchi, G. Tagliabue,
A. Sironi, J. A. R. Navarro, J. M. Salas,
L. Mendez-Liñan, M. Domingo,
M. Perez-Mendoza, E. Barea*

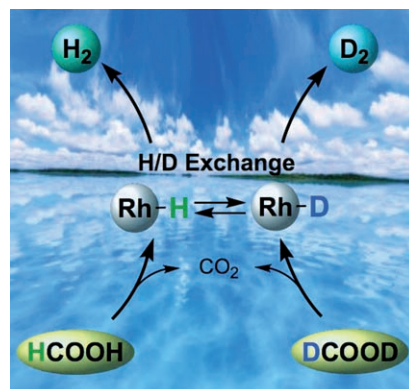
Polymorphic Coordination Networks Responsive to CO₂, Moisture, and Thermal Stimuli: Porous Cobalt(II) and Zinc(II) Fluoropyrimidinates

Chem. Eur. J.

DOI: 10.1002/chem.200801048

Forming formate and generating gas:

The water-soluble rhodium aqua complex $[\text{Rh}^{\text{III}}(\text{Cp}^*)(\text{bpy})(\text{H}_2\text{O})]^{2+}$ efficiently and selectively catalyzes the decomposition of formic acid to H₂ and CO₂ in aqueous solution at 298 K. Hydrogen evolution occurs through formation of the formate complex, $[\text{Rh}^{\text{III}}(\text{Cp}^*)\{\text{OC}(\text{O})\text{H}\}(\text{bpy})]^{+}$, followed by a rate-determining β -hydrogen elimination to afford the hydride complex, $[\text{Rh}^{\text{III}}(\text{Cp}^*)(\text{H})(\text{bpy})]^{+}$, the catalytic active species.



Hydrogen Generation

S. Fukuzumi,* T. Kobayashi, T. Suenobu

Efficient Catalytic Decomposition of Formic Acid for the Selective Generation of H₂ and H/D Exchange with a Water-Soluble Rhodium Complex in Aqueous Solution

ChemSusChem

DOI: 10.1002/cssc.200800147